Analysis of dielectric circular cylinder light spot narrowing by whispering gallery modes and influence of material absorption

D.A. Kozlov[1,2], E.S. Kozlova[1,2], V.V. Kotlyar[1,2]

[1]Image Processing Systems Institute of RAS - Branch of the FSRC "Crystallography and Photonics" RAS, Molodogvardejskaya street 151, Samara, Russia, 443001
[2]Samara National Research University, Moskovskoe Shosse 34A, Samara, Russia, 443086

Abstract. We present results of numerical analysis of the diffraction of a plane monochromatic TE-wave on an ideal homogeneous dielectric cylinder with several resonant wavelength scale radii. Two subsequent near-surface maxima of intensity (two focuses) generated at the cylinder output were found on the optical axis. The first subwavelength focus is formed by one of the whispering gallery mode lobes. Its intensity is 50 times the incident light intensity and its full width at the half maximum of the intensity is equal to 0.155 of the incident wavelength. The second focus is two times less in intensity. Its focal spot known as a photonic nanojet is stretched toward the optical axis. The second focus is formed at a distance about the wavelength from the cylinder surface. Its width is equal to 0.44 of the wavelength and its length is two wavelengths. The influence of material absorption on the light focusing is also examined by numerical simulation.

Keywords: Dielectric cylinder, whispering gallery modes, subwavelength focusing.

1. Introduction

Subwavelength light focusing (focusing into a region with dimensions smaller than the wavelength) by microparticles and small obstacles which sizes as a rule are comparable to wavelengths is a comparatively new area of scientific research. This physical phenomenon attracts attention after publications [1–3]. It was shown [1] that a dielectric microsphere focus light into a rather narrow spot (known as a photonic nanojet). If there is a nanoparticle inside the photonic nanojet the scattered field detects this object. Nanojets are typically formed by diffraction gratings [4] and radially symmetric obstacles [5] and a gradient lenses [6]. Several papers is devoted to light focusing by a multilayered microsphere [7], a spheroidal microsphere [8], a two-layered microsphere [9, 10], a cylinder [11-13], and a disk [14]. Since sharp focusing allows to increase resolutions of microscopes and optical detectors, the basic application of sharp focusing is probing and detecting of nanoobjects. Resonant modes can be excited in all the above-mentioned microobjects. For example, the excitation of the 18-th whispering gallery mode in a microcylinder from polyester was examined [15]. Optical resonances in particles and microobjects are used in highly sensitive sensors and filters [16]. The quality factors of optical resonance modes are extremely high [17] and, consequently, their spectral widths are very

narrow. It allows to use them in supersensitive filters. Optical resonances are used to obtain subwavelength focusing of light since transverse sizes of focal spots decrease when resonant modes are excited inside the optical element [18–20].

In this paper the whispering gallery modes and their influence on the subwavelength light focusing are investigated by using the existing analytical solution of the diffraction problem on a cylinder. We have improved our results [19] reducing the width of the focal spot to 0.155 of the wavelength. We also discuss the subwavelength focusing and whispering gallery modes in a two-layered cylinder. It is shown that taking into account the complex refractive index, i.e. taking into account the material absorption, leads to a substantial weakening of the whispering gallery modes and their influence on the light focusing.

2. Analysis of whispering gallery modes

In our previous paper [19, 20] the method was shown which allows to achieve focusing of TE-polarized radiation in a region that is more than two times smaller than the diffraction limit in the two-dimensional case (the focus full width at the half maximum of the intensity was FWHM = 0.44 λ). This result can be obtained only when the radius of the cylinder is in a certain relation to the wavelength. The 30-th resonant mode excited by irradiation with monochromatic light in the cylinder with the refractive index $n = 1.5875$ (refractive index of the external medium n=1) is amplified if the ratio between the radius of the cylinder and the wavelength is $R = 3.4745041\ \lambda$ (the width of the resonance was equal to $\Delta R = 3.4\times10^{-5}\ \lambda$). The value of this ratio can be obtained with an arbitrary accuracy by using approximate formula [2] or an optimization algorithm. If this relationship is satisfied, alternating maxima and intensity minima are formed on the cylinder boundary. An isolated maximum on the optical axis at the shadow side of the cylinder can be interpreted as a focal spot generated by the cylinder. The values of FWHMs (the focus full widths at the half maximum of the intensity in the direction perpendicular to the light propagation direction) of 25th – 65th modes were calculated in terms of the wavelength λ up to the third decimal place (figure 1). The intensity is calculated as the squared modulus of the amplitude of the electric field strength. Figure 1 shows three curves obtained for three different values of polyester refractive indices: $n = 1.5875$ (for the wavelength of the helium-neon laser λ = 632,8 nm), $n = 1.6010$ (for the the wavelength of the argon laser λ = 514 nm), and $n = 1.6117$ (for the wavelength of the argon laser λ = 488 nm) [21].

It is should be noticed that all the values of the FWHM are obtained using our analytical solution of the problem of a plane monochromatic TE-wave diffraction by a homogeneous dielectric cylinder. Firstly, it can be seen from figure 1 that the minimal size of the focal spot is equal to $(0.155 \pm 0.001)\lambda$. This value can be achieved while focusing the 60-th mode ($n = 1.5875$) by the cylinder with radius of $R = 6.63186178877\ \lambda$ ($\Delta R = 4.0\times10^{-10}\ \lambda$). Secondly, the resonant mode with number $m = 60$ is of interest itself since for this mode the focal spot at the boundary of our cylinder has the minimal size. In figure 1, we see that the curve of FWHM has a sharp local minimum. The two-dimensional distribution of the intensity near the focus for this mode ($m = 60$) is shown in figure 2. It can be seen that there are three additional spots near a small central spot (the left vertical white line segment) generated at the boundary of the cylinder. One of them is the photonic nanojet and two other spots are lobes formed as a result of interference of the transmitted light and the mode generated in the cylinder. The intensity of the central maximum is 50 times intensity of the incident light. However, the intensity of the neighbouring lobes exceeds the intensity of the incident light only twice (figure 3a). The intensity in the photonic nanojet maximum (the right vertical white line segment) more than 2 times less incident intensity (figure 3b).

The photonic nanojet is the region of the second focus on the optical axis. Its maximum is formed at the distance of 0.87 λ from the surface of the cylinder and its width and depth are equal to 0.44 λ and 2 λ respectively.

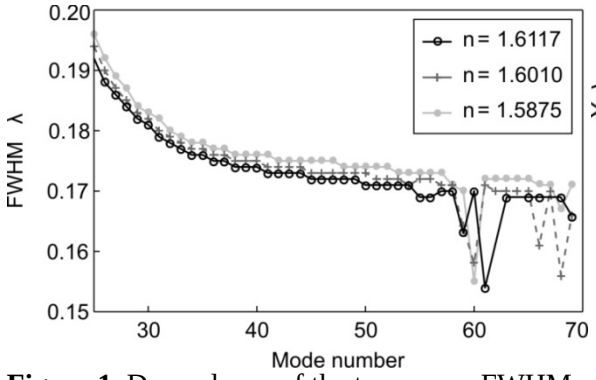

Figure 1. Dependence of the transverse FWHM of focal spot on the excited in the cylinder mode number.

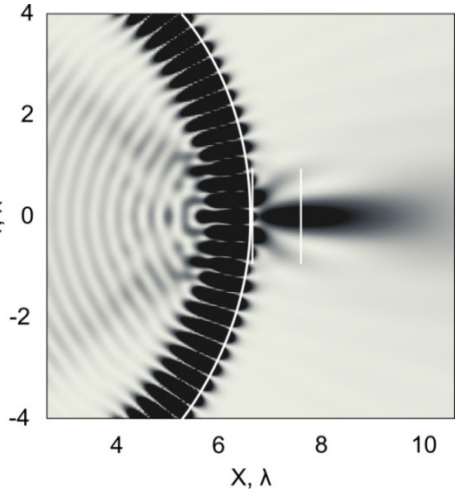

Figure 2. Two-dimensional negative distribution of light intensity near cylinder inside of which 60-th whispering gallery mode is generated.

Some points are omitted in figure 1. The reason is that a focal spot at the boundary of the cylinder is generated not for the all resonances. For example, figure 4b shows the distribution of intensity of the 62-th mode in polyester cylinder with $n = 1.6117$, $R = 6.7391161\ \lambda$, $\Delta R = 2\times10^{-11}\ \lambda$. In this resonance case, there is no focus at the surface on the optical axis (the left white dashed line in figure 4b). This fact suggests that not all modes with numbers greater than 50 are stable, i.e. not all modes are held within the cylinder as well as, for example, the mode with the number 30 presented in figure 4a. First of all it is indicated by a lower value of the maximal intensity at the boundary of the cylinder. Indeed, the intensity in the lobes of the mode is much less than the intensity of the mode in figure 4a. It is comparable with the intensity in the photonic nanojet (the right dashed vertical white line in figure 4b).

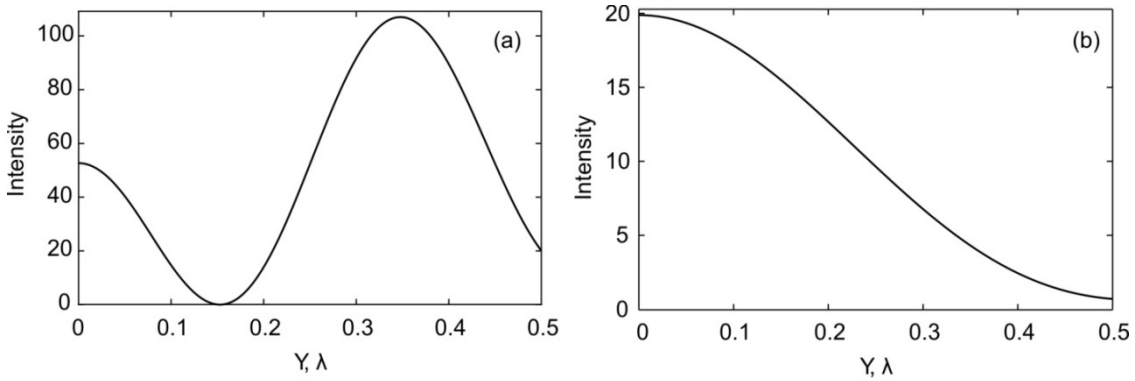

Figure 3. Distribution of intensity from centre of symmetry perpendicular to optical axis in cross-section at the boundary of cylinder (a) and at distance of 0.86 λ from its surface (b).

3. Influence of absorption on resonant focusing

In the previous sections, the intensities used to define the FWHM were calculated for ideal non-absorbing materials. In our analytical solution, absorption can be taken into account to find out how it affects the resonances. In addition, the minimal size of the focal spot which can be obtained in materials with real absorption coefficient can be defined.

Unfortunately, there are only few works concerned with the absorption of polyester. We can mention the paper [22] where the authors investigated optical properties of polyester in infrared region and the paper [23] concerned with measuring of the imaginary part of the polyester refractive index covering the range from visible to X-ray. Only estimation of the upper boundary of the absorption

coefficient (the imaginary part of the complex refractive index) can be got from this papers. Approximately, it is equal to $1.0\times10^{-3} – 2.5\times10^{-3}$. In paper [24] optical properties of thin films from the iodine-doped polyester and from pure polyester are compared. We are interested in the wavelength 632.54 nm of the helium-neon laser for which the imaginary part of the refractive index is $1.1\times10^{-3} – 1.2\times10^{-3}$.

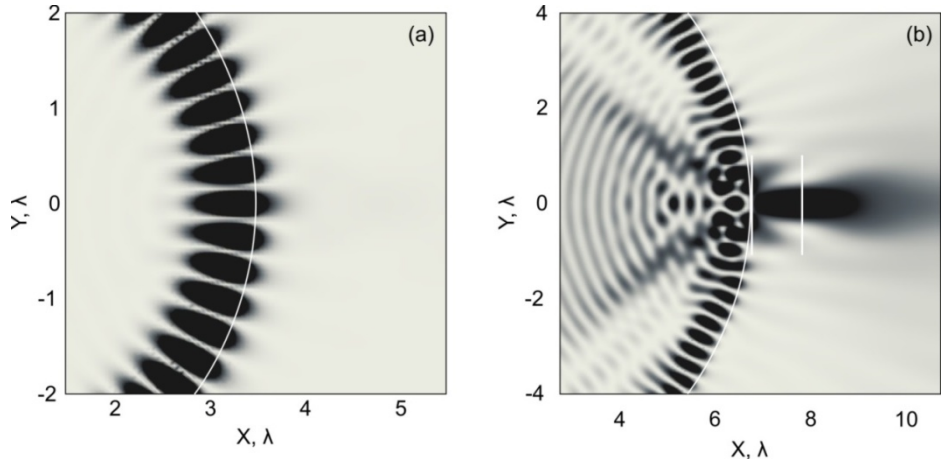

Figure 4. Two-dimensional negative distributions of light intensity near boundaries of cylinders inside of which 30-th (a) and 62-th (b) whispering gallery modes are generated.

The absorption coefficient can be reduced significantly using the doped material. In paper [25] the parameters of polyester irradiated by ions Ar++ and H+ in the visible light spectrum is presented. At the wavelength of the helium-neon laser, the imaginary part of the refractive index reaches the value $k = 2.73\times10^{-7}$ after irradiating by ions H+ with the energy 200 keV (the minimal concentration). When polyester was irradiated by ions Ar++ with the energy 400 keV the absorption coefficient $k = 2.54\times10^{-5}$ is obtained.

The dependences of the maximal intensities inside the focal spot on k was calculated to estimate the influence of material absorption on the focal spot size and to define the conditions of resonant mode generation. The results are presented in figures 5 and 6 for the 60-th and the 30-th modes, respectively.

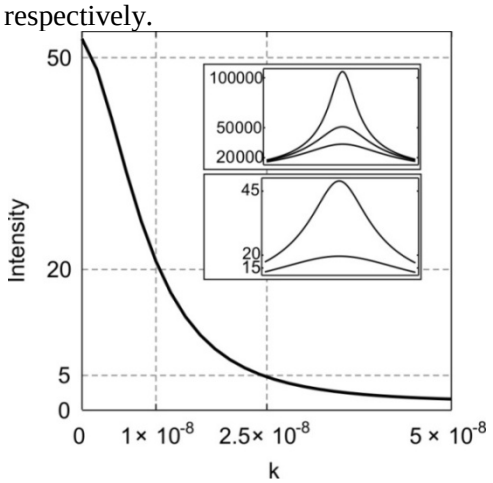

Figure 5. Maximal intensity on optical axis at boundary of cylinder in which 60-th mode is excited: the inserts show the dependence of the mode coefficient in expansion on cylindrical functions near the resonance value for different values of the refractive index from top to bottom: $k = 0$, $k = 0.5\times10^{-11}$, $k = 10^{-11}$, $k = 10^{-8}$, $k = 2.5\times10^{-8}$, respectively.

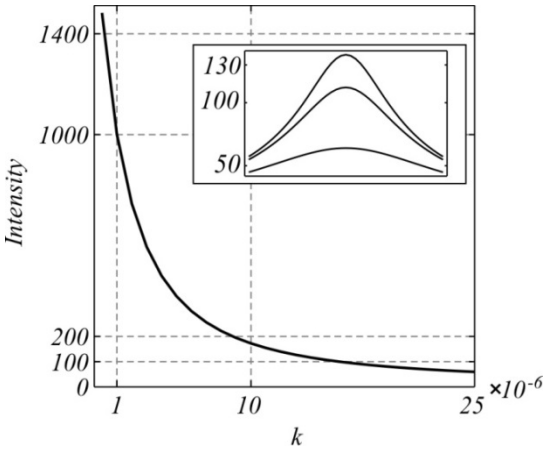

Figure 6. Maximal intensity on optical axis at boundary of cylinder in which 30-th mode is excited: the inserts show the dependence of the mode coefficient in expansion on cylindrical functions near the resonance value for different values of the refractive index from top to bottom: $k = 0$, $k = 10^{-6}$, $k = 5\times10^{-6}$, respectively.

It can be seen from figure 5 that it is impossible to get the distribution of intensity as in figure 2 while the absorption coefficient is close to its value for polyester. Even when $k = 2.5\times10^{-8}$ the intensity in the focus at the boundary of the cylinder falls by an order of magnitude. There is no focal spot for the larger values of the absorption coefficient because the difference between the first order interference minimum and maximum becomes hardly distinguishable. The resonance itself remains in the presence of absorption, but it is much worse. It can be seen from inserts of figure 5 and figure 6 that the maximum of the coefficient in the expansion by modes does not shift, however it decreases by five orders of magnitude for the 60-th mode even when $k = 10^{-8}$. Thus a focus could not be obtained for the 60-th mode even using specific materials discussed above. The mode with the number 30 can be obtained with the value of the absorption coefficient up to $k = 1\times10^{-5}$ and the minimal focus size FWHM = 0.18 λ is obtained for the absorption coefficient $k = 2.73\times10^{-7}$. Figure 7 shows the dependence of FWHM (mode number 30) on the absorption coefficient. It can be seen from this figure that FWHM increases with increasing of the material absorption.

Due to absorption, mode becomes less stable inside the cylinder and "flow away" from it quicker. However, this does not always lead to increasing of FWHM of focal spot at the cylinder boundary. Figure 8 shows the dependence of the transverse size of the focal spot on the mode number for analogous parameters as at figure 1 and $k = 2.73\times10^{-7}$. It can be seen from figure 10 that increasing of absorption leads to substantial decreasing of FWHM of focal spot at the cylinder boundary for numbers of the modes larger than 40. As an example, the distribution of the intensity of the 48-th is shown in figure 8. The size of the only slightly protruding maximum of the intensity on the optical axis at the boundary of cylinder is FWHM = 0.138 λ. It worth to be mentioned that the distribution of the intensity almost coincide with the one presented on figure 2, however figure 2 corresponds to the case of zero absorption.

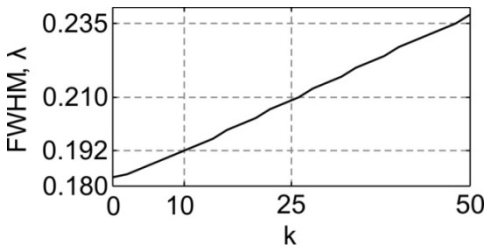

Figure 7. Maximal intensity on optical axis at boundary of cylinder in which 60-th mode is excited: the inserts show the dependence of the mode coefficient in expansion on cylindrical functions near the resonance value for different values of the refractive index from top to bottom: $k = 0$, $k = 0.5\times10^{-11}$, $k = 10^{-11}$, $k = 10^{-8}$, $k = 2.5\times10^{-8}$, respectively.

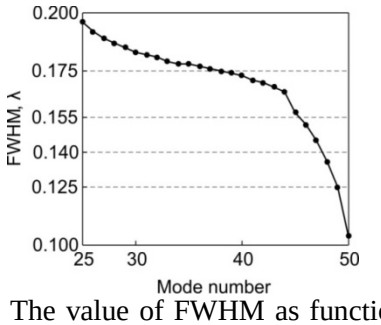

Figure 8. The value of FWHM as function of generated mode number for $k = 2.73\times10^{-7}$.

4. Conclusion

In the present paper, we numerically calculated with high accuracy the minimal size of the focal spot in the case of plane TE-polarized waves diffracted by homogeneous ideal cylinders from polyester with resonant radii. In this case the FWHM of focal spot is equal to $(0.155 \pm 0.001)\lambda$. Absorption from one hand prevents sharp focusing of the light but from the other hand it allows us to obtain smaller sizes of the focal spot. For example, the focal spot with FWHM = 0.138λ is formed in the case of 48-th resonance mode generated in the cylinder from polyester with refractive index as $n + ik = 1.5875 + 2.73\times10^{-7}i$. Our results can form the basis for developing new optical elements for optical tweezers [26, 27], ultra-sensitive sensors [16], and systems of optical recording and storage of information [28].

5. Acknowledgements

This work was supported by the Federal Agency of Scientific Organizations (agreement No 007-ГЗ/Ч3363/26) and the Ministry of Education and Science of the Russian Federation (# SP-4375.2016.5), a RF Presidential grants for support of leading scientific schools (NSh-6307.2018.8) and young candidate of science (MK-9019.2016.2),and the Russian Foundation for Basic Research (##17-47-630420, 17-47-630417, 16-47-630483, 15-07-01174).

6. References

[1] Chen, Z. Photonic nanojet enhancement of backscattering of light by nanoparticles: a potential novel visible-light ultramicroscopy technique / Z. Chen, A. Taflove, V. Backman // Opt. Exp. – 2004. – Vol. 12(7). – P. 1214-1220.

[2] Kozlova, E.S. Simulation of the resonance focusing of picosecond and femtosecond pulses by use of a dielectric microcylinder / E.S. Kozlova, V.V. Kotlyar // Computer Optics. – 2005. – Vol. 39(3). – P. 319-232.

[3] Kotlyar, V.V. Photonic nanojets formed by square mircosteps / V.V. Kotlyar, S.S. Stafeev, A.Yu. Feldman // Computer Optics. – 2015. – Vol. 18(1). – P. 72-80.

[4] Geints, Y.E. Modeling spatially localized photonic nanojets from phase diffraction gratings / Y.E. Geints, A.A. Zemlyanov // J. Appl. Phys. – 2016. – Vol. 119(15). – P. 153101.

[5] Geints Y.E. Localized light jets from radially symmetric nonspherical dielectric microparticles / Y.E. Geints, A.A. Zemlyanov, E.K. Panina // Atmospheric and Oceanic Optics. – 2015. – Vol. 28(5). – P. 436-440.

[6] Mao, X. Tunable photonic nanojet formed by generalized Luneburg lens. / X. Mao, Y. Tang, H. Dai, D. Luo, D. Yao, Sh. Yan // Opt. Exp. – 2015. – Vol. 23(20). – P. 26426-26433.

[7] Geints, Y.E. Photonic nanojet calculations in layered radially in homogeneous micrometer-sized spherical particles / Y.E. Geints, A.A. Zemlyanov, E.K. Panina // J. Opt. Soc. Am. B. – 2011. – Vol. 28(8). – P. 1825-1830.

[8] Han, L. Photonic jet generated by spheroidal particle with Gaussian-bean illumination / L. Han, Y. Han, G. Gouesbet, J. Wang, G. Grehan // J. Opt. Soc. Am. B. – 2014. – Vol. 31(7). – P. 1476-1483.

[9] Grojo, D. Bessel-like photonic nanojets from core-shell sub-wavelength spheres / D. Grojo, N. Sandeau, L. Boarino, C. Constantinescu, N. De Leo, M. Laus, K. Sparnacci // Opt. Lett. – 2014. – Vol. 39(13). – P. 3989-3992.

[10] Shen, Y. Ultralong photonic nanojets formed by a two-layers dielectric microsphere / Y. Shen, L.V. Wang, J. Shen // Opt. Lett. – 2014. – Vol. 39(14). – P. 4120-4123.

[11] Gu, G. Super-long photonic nanojet generated from liquid-filled hollow mircocylinder / G. Gu, R. Zhou, Z. Chen, H. Xu, G. Cai, M. Hong // Opt. Lett. – 2015 – Vol. 40(4) – P. 625-628.

[12] Liu, C. Photonic nanojet modulation by elliptical microcylinders / C. Liu, L. Chang // Optik. – 2014. – Vol. 125(15). – P. 4043-4046.

[13] Xu, B.B. Cui Annular focusing lens based on transformation optics / B.B. Xu, G.X. Jiang, T.J. Yu // J. Opt. Soc. Am. A. – 2014. – Vol. 31(5). – P. 1135-1140.

[14] Wangm, J.J. Low divergence photonic nanojets from Si3N4 mircodisks / J.J. Wangm, J.F. Donegan // Opt. Exp. – 2012. – Vol. 20(1). – P. 128-140.

[15] Kozlova, E.S. Modeling the resonance focusing of a pico-second laser pulse using a dielectric microcylinder / E.S. Kozlova, V.V. Kotlyar, S.A. Degtyarev // J. Opt. Soc. Am. B. – 2015. – Vol. 32(11). – P. 2352-2357.

[16] Foreman, M.R. Whispering gallery mode sensors / M.R. Foreman, J.D. Swaim, F. Vollmer // Advances in Optics and Photonics. – 2015. – Vol. 7(2). – P. 168-240.

[17] Gorodetsky, M.L. Ultimate Q of optical microsphere resonators / M.L. Gorodetsky, A.A. Savchenkov, V.S. Ilchenko // Opt. Lett. – 1996. – Vol. 21(7). – P. 453-455.

[18] Geints, Y.E. Photonic jets from resonantly exited transparent dielectric microspheres / Y.E. Geints, A.A. Zemlyanov, E.K. Panina // J. Opt. Soc. Am. B. – 2012. – Vol. 29(4). – P. 758-762.

[19] Kozlov, D.A. Resonant laser focus light by uniformity dielectric mircocylinder / D.A. Kozlov, V.V. Kotlyar // Computer Optics. – 2014. – Vol. 38(3). – P. 393-396.

[20] Kotlyar, V.V. Calculating the resonance radius of a dielectric cylinder under illumination by a plane TE-wave / V.V. Kotlyar, A.A. Kovalev, D.A. Kozlov // Optik. – 2016. – Vol. 127(8). – P. 3803-3808.
[21] Soifer, V.A., Diffractive nanophotonics / V.A. Soifer– Moscow: Francis, London, 2011.
[22] Simon, J. Determination of optical constants of polystyrene from IR reflection-absorption spectra / Simon J. // Analele Universităţii Eftimie Murga Reşiţa. – 2011. –Vol. 18(1). – P. 41-48.
[23] Inagaki, T. Optical properties of polystyrene from the near-infrared to the X-ray region and convergence of optical sum rules / T. Inagaki, E.T. Arakawa, R.N. Hamm, M.W. Williams // Phys. Rev. B: Condens. Matter. – 1997. – Vol. 15(6). – P. 3243-3253.
[24] Sharma, D. Comparison of optical properties of spun cast polystyrene and iodine doped films / D. Sharma, P. Sharma, K.R. Singh, N. Thakur // Optoelectronics and advanced materials: Rapid communications. – 2009. – Vol. 3(4). – P. 371-375.
[25] Kanuchova, Z. Space weathering of asteroidal surfaces. Influence on the UV-Vis spectra / Z. Kanuchova, G.A. Baratta, M. Grozzo, G. Strazzulla // Astronomy & Astrophysics. – Vol. 517(A60).
[26] Porfirev, A.P. Optical capture of microparticles in special traps / A.P. Porfirev, R.V. Skidanov // Computer Optics. – 2012. – Vol. 36(2). – P. 211-218.
[27] Soifer, V.A. Optical microparticle manipulation: advances and new possibilities created by diffractive optics / V.A. Soifer, V.V. Kotlyar, S.N. Khonina // Physics of Particles and Nuclei. – 2004. – Vol. 35(6). – P. 733-766.
[28] Li, X. Multifocal optical nanoscopy for big data recording at 30 TB capacity and gigabits/second data rate / X. Li, Y. Cao, N. Tian, L. Fu, M. Gu // Optica. – 2015. – Vol. 2(6). – P. 567-570.